Dynamic Gas Flow Effects on the ESD of Aerospace Vehicle Surfaces

Michael D. Hogue, PhD
NASA, Flight Technology Branch, UB-R2
Electrostatics & Surface Physics Laboratory
Kennedy Space Center, FL 32899
phone: (1) 321-867-7549
E-mail: Michael.D.Hogue@nasa.gov

Jayanta Kapat, PhD
University of Central Florida
Orlando, FL 32816
E-mail: Jayanta.Kapat@ucf.edu

Kareem Ahmed, PhD
University of Central Florida
Orlando, FL 32816
E-mail: Kareem.Ahmed@ucf.edu

Rachel E. Cox
NASA, Flight Technology Branch, UB-R2
Kennedy Space Center, FL 32899
E-mail: Rachel.E.Cox@nasa.gov

Jennifer G. Wilson
NASA, Flight Technology Branch, UB-R2
Kennedy Space Center, FL 32899
E-mail: Jennifer.G.Wilson@nasa.gov

Luz M. Calle, PhD
NASA, Applied Science Branch, UB-R3
Kennedy Space Center, FL 32899
E-mail: Luz.M.Calle@nasa.gov

Jaysen Mulligan
University of Central Florida
Orlando, FL 32816
E-mail: mulligan2015@gmail.com

Abstract— **The purpose of this work is to develop a version of Paschen's Law that takes into account the flow of ambient gas past electrode surfaces. Paschen's Law does not consider the flow of gas past an aerospace vehicle, whose surfaces may be triboelectrically charged by dust or ice crystal impingement while traversing the atmosphere. The basic hypothesis of this work is that the number of electron-ion pairs created per unit distance between electrode surfaces is mitigated by the electron-ion pairs removed per unit distance by the flow of gas. The revised theoretical model must be a function of the mean velocity, v_{xm}, of the ambient gas and reduce to Paschen's law when the gas mean velocity, v_{xm} = 0. New theoretical formulations of Paschen's Law, taking into account Mach number and dynamic pressure, derived by the authors, will be discussed. These equations will be evaluated by wind tunnel experimentation later this year. Based on the results of this work, it is hoped that the safety of aerospace vehicles will be enhanced with a redefinition of electrostatic launch commit criteria. It is also possible that new products, such as anti-static coatings, may be formulated from this data.**

TABLE 1: NOMENCLATURE

α	Electron – ion pairs created per unit length
α'	Electron – ion pairs created per unit length with gas flow
β	Electron – ion pairs removed per unit length by the gas flow
δ	Electron – ion pairs added per unit length by the gas flow
V_s	Sparking discharge voltage (V)
P	Gas pressure (torr)
P_0	Ambient gas pressure (torr)
P_D	Dynamic pressure (torr)
c	Speed of sound (319 m/s at sea level)
q_e	Electron charge (1.602×10^{-19} Coulomb)
d	Electrode separation (cm)
d'	Effective electrode separation due to gas flow (cm)
P_{atm}	Atmospheric pressure at sea level (760 torr)
L	Mean free path at sea level (6.8×10^{-6} cm)
γ	Secondary electron emission coefficient
v_{xm}	Mean velocity of the ambient gas (m/s)
n_e	Number of electrons
n_i	Number of ions
n	Number of moles
E	Electric field (V/m)
$\forall$	Volume (m^3)
R	Universal gas constant (8.314 J/K·mol)
M	Molecular weight of the gas (kg/mol)
W	Mass of the gaseous phase (kg)
ρ	Density (kg/m^3)
T	Temperature (K)
γ_a	Ration of specific heat at constant pressure to the specific heat at constant volume of the mediating gas.

I. INTRODUCTION

We have developed modified versions of Paschen's law [1] that take into account the flow of gas between electrically charged conductive plates. This work is applicable to aerospace vehicles traveling through the atmosphere where they are subject to triboelectrically induced electrostatic charge build-up and possible electrostatic discharge (ESD) damage due to dust and ice crystal impingement. We will then validate the theoretical result by wind tunnel experimentation at supersonic gas velocities to model aircraft and spacecraft moving through the atmosphere.

In 2010, the Electrostatics and Surface Physics Laboratory (ESPL) at the Kennedy Space Center (KSC) performed an analysis to determine if ice crystal impingement on the exterior of the Ares I self-destruct system antenna housing would cause any electrostatic interference on the operation of the antenna [2]. In the course of the analysis, the ESPL estimated at what potential a discharge could occur if the housing was charged triboelectrically by the ice crystals at altitudes where the ambient pressure is less than that at sea level. The difficulty in doing this was that Paschen's law was derived for stationary charged surfaces in ambient gas that had no net velocity. This was not a very good fit for the physical situation of a vehicle moving rapidly through the atmosphere where the electron-ion pairs created by the electrostatic potential can be quickly removed by the gas flow. The safety of the housing to electrostatic discharge damage was eventually shown by extensive laboratory testing despite there being no appropriate theoretical model to use.

This work has the potential to relax the launch criteria for triboelectric charging due to atmospheric dust or ice crystal impingement on spacecraft surfaces. This would save considerable sums of money (ROM of around a million U.S. dollars) on launch costs if a launch scrub could be avoided. Also, better antistatic coatings may be developed based on the results of this work.

II. THEORETICAL DEVELOPMENT

In this section we describe Paschen's Law and the derivation of three candidate theoretical Paschen's Law equations. An initial formulation using Reynold's number was attempted first but was found to be nonviable. The first candidate equation is developed using the Mach number while the second uses the Mach number with the addition of dynamic pressure terms [3]. The third model equation incorporates dynamic pressure terms only.

A. Paschen's Law

Paschen's law, derived in 1889 [1], is an equation that relates the sparking or breakdown voltage between two electrodes to the product of the ambient gas pressure, P, and the electrode separation, d. When the sparking voltage, V_s, is reached, a discharge occurs between the electrodes. Other constant parameters in Paschen's law are the ionization potential of the ambient gas, V_i, atmospheric pressure at sea level, P_{atm}, molecular mean free path at sea level, L, and the secondary electron emission coefficient of the electrode material, γ. Paschen's law is shown in Eq. (1) below [4]. As the electric potential builds up between the electrodes, it affects the small number of electrons and ions typically present in the air (electron-ion pairs). These particles then separate and move towards the oppositely

charged electrode. On the way, they can strike and ionize other atoms and molecules thus creating a cascade of charged particles that eventually results in an electrostatic or sparking discharge between the electrodes.

$$V_s = \frac{\frac{V_i}{LP_{atm}}Pd}{ln(Pd) - ln\left[LP_{atm} ln\left(1+\frac{1}{\gamma}\right)\right]} \qquad (1)$$

Our hypothesis is that the number of electron-ion pairs created per unit distance is mitigated by the electron-ion pairs removed per unit distance by the flow of gas past the electrodes. In this first approximation, we treat the pressure gradient along the vertical axis (perpendicular to the flow) as a constant. The modified equation must be a function of the mean velocity, v_{xm}, of the ambient gas and reduce to Paschen's law, Eq. (1), when $v_{xm} = 0$.

B. Mach Number Formulation

When an electric potential difference is set up between two electrodes, neutral gas atoms and molecules can become ionized by collisions with the ions typically present in air. These electron-ion pairs then separate with the electrons traveling toward the positive electrode and the positively charged ions moving toward the negative electrode. If the velocity of these charged particles is great enough (kinetic energy of $K \geq q_e V_i$), then other atoms and molecules will become ionized. These new electron-ion pairs will then separate and collide with other neutral particles creating what is called a cascade of charged particles rendering the mediating gas between the electrodes more conductive. This process will eventually lead to an electrostatic or sparking discharge between the electrodes.

The number of new electron-ion pairs, dn, can be calculated by [4]

$$\mathrm{d}n = n\alpha \mathrm{d}x \qquad (2)$$

The ionization coefficient, α, is defined as the number of electron-ion pairs created per unit distance. For flowing gas, we need to define coefficients that deal with the removal and addition of electron-ion pairs from the vicinity of the electrodes. We define β as the electron-ion pairs per unit distance lost and δ as the electron-ion pairs per unit distance added by the gas flow. This changes equation (2) to

$$\mathrm{d}n = n(\alpha - \beta + \delta)\mathrm{d}x = n\alpha' \mathrm{d}x \qquad (3)$$

Unless the ambient gas is ionized to begin with, we can neglect the effect of the δ term so Eq. (3) can be simplified.

$$\mathrm{d}n \cong n(\alpha - \beta)\mathrm{d}n \cong n\alpha' \mathrm{d}x \qquad (4)$$

Separating variables, integrating over the separation of the electrodes (from 0 to d), and solving for the number of electrons, n_e, we have

$$\int_1^{n_e} \frac{\mathrm{d}n}{n} = \alpha' \int_0^d \mathrm{d}x$$

$$n_e = e^{\alpha' d} \tag{5}$$

For the number of ions, n_i, we subtract one from the number of electrons.

$$n_i = e^{\alpha' d} - 1 \tag{6}$$

When positive ions strike the cathode, other electrons are released and travel to the anode. The probability per ion that electrons are released is the secondary electron emission coefficient of the electrode material, γ. A self-regenerative breakdown condition is Townsend's regeneration condition [4]

$$\gamma\left(e^{\alpha' d} - 1\right) = 1 \tag{7}$$

Solving Eq. (7) for α' we get

$$\alpha' = \frac{1}{d} ln\left(\frac{1}{\gamma} + 1\right) \tag{8}$$

There are two basic assumptions required to derive Paschen's law. One, each electron, traveling a distance ($0 \le l \le d$) through an electric field E between the electrodes, loses all of its kinetic energy on impact with other particles. Two, each electron can ionize a neutral particle when its kinetic energy, $q_e El$, (where q_e is the charge on the electron, 1.602×10^{-19} Coulomb) is equal to or greater than the ionization energy, $q_e V_i$, of the mediating gas.

To get an energy $q_e V_i$, an electron must travel a distance y_i. The probability of this is given by [4]

$$e^{-\frac{y_i}{l}} = e^{-\frac{V_i}{El}} \tag{9}$$

where $1/l$ is the number of impacts per unit distance.

Our hypothesis is that the probability of the loss of electron ion pairs around the electrodes by the gas flow is given by a dimensionless aerodynamic term that is proportional to the gas velocity. The candidate aerodynamic function we used for this derivation is the Mach number, $M_N = v_{xm}/c$ where v_{xm} is the mean gas velocity and c is the speed of sound. The Mach number was chosen because it is a function of the gas velocity and is dimensionless. The number of electron-ion pairs formed per unit distance and those removed by the gas flow can be determined by Eq. (9) with the addition of a Mach number term.

$$\alpha' = \frac{1}{l} e^{-\frac{V_i}{El} - M_N} \tag{10}$$

The E-field at discharge is $E = V_s/d$ and we substitute this into Eq. (10) to get

$$\alpha' = \frac{1}{l} e^{-\frac{V_i d}{V_s l} - M_N} \tag{11}$$

Using $l = LP_{atm}/P$ and setting Eqs. (8) and (11) equal and solving for the discharge or sparking voltage we get

$$V_s = \frac{\frac{V_i}{LP_{atm}}(Pd)}{ln(Pd) - ln\left[LP_{atm} ln\left(1+\frac{1}{\gamma}\right)\right] - M_N} \tag{12}$$

This theoretical model, Eq. (12), is Paschen's Law, Eq. (1), with the Mach number in the denominator. This equation meets the requirement that when $v_{xm} = 0$ it reverts to Paschen's Law.

A graph of Eq. (12) and Paschen's Law is shown in Fig. 1 for T6061 Aluminum electrodes ($\gamma = 0.035$ [5]) with an air velocity of 600 m/s (Mach 1.9) and an electrode gap of 1.0 cm.

As can be seen in Fig. 1, the addition of the Mach number to modify the number of electron – ion pairs created between the electrodes increases the resulting sparking voltage. The effect is more pronounced at lower values of *Pd*.

C. Mach number Formulation with Dynamic Pressure

In fluid flow, pressure has two components. One is the static or ambient pressure, P_0, and a dynamic pressure, P_D, due to the flow of gas [3]. We can write the dynamic pressure in terms of the mean gas velocity as

$$P_D = \frac{1}{2}\rho v_{xm}^2 \tag{13}$$

where ρ is the fluid density. This gives for the total pressure on a surface

$$P = P_0 + P_D = P_0 + \frac{1}{2}\rho v_{xm}^2 \tag{14}$$

Treating the air as an ideal gas we have

$$P_0 \forall = nRT \tag{15}$$

The symbol $\forall$ is volume (to differentiate it from velocity and voltage), n is the number of moles, R is the universal gas constant (8.314 J/K·mol), and T is the temperature in Kelvin. We can also write Eq. (15) in terms of the molecular weight of the gas, M.

$$P_0 \forall = \left(\frac{W}{M}\right) RT \tag{16}$$

Here $W = nM$ and is the mass of the gaseous phase. We can write equation (16) in terms of density by

$$\frac{P_0 M}{RT} = \frac{W}{\forall} = \rho \tag{17}$$

This gives in Eq. (14)

$$P = P_0 + \frac{1}{2}\frac{P_0 M}{RT} v_{xm}^2 = P_0\left(1 + \frac{1}{2}\frac{M}{RT} v_{xm}^2\right) \tag{18}$$

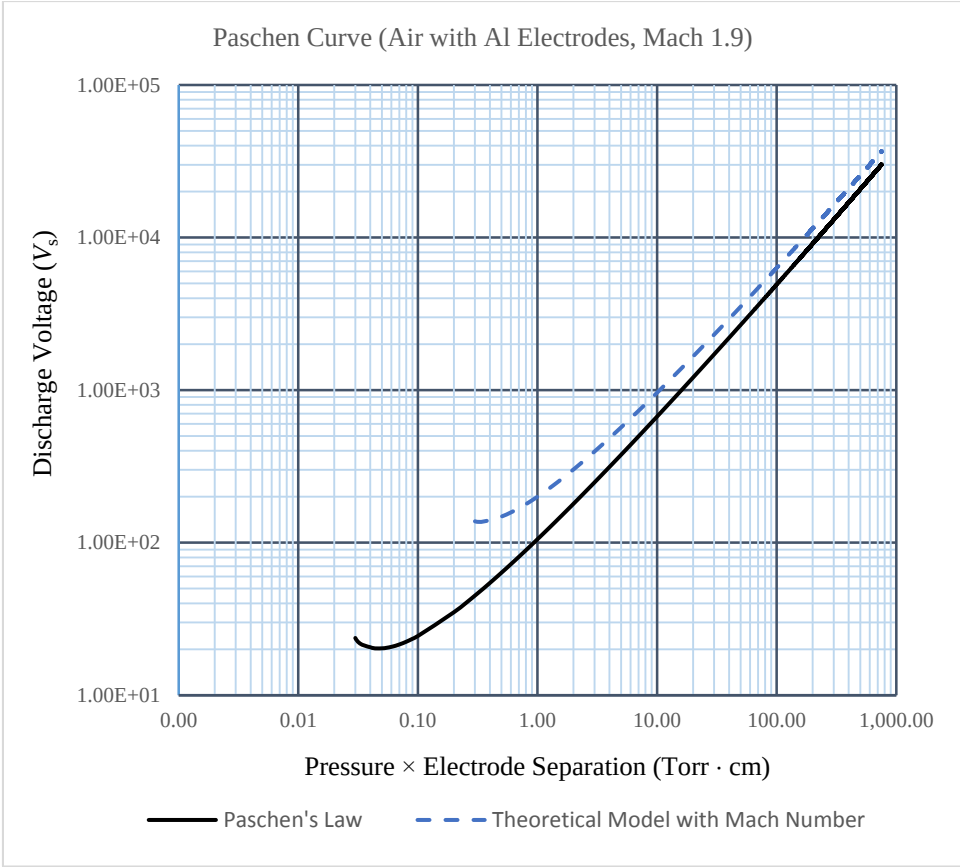

Figure 1. Paschen's Law curve compared to the theoretical model with Mach number formulation for Aluminum electrodes in air moving at Mach 1.9.

We assume that the gas compressibility factor, Z is ≈ 1. Incorporating Eq. (18) into Eq. (12) and rearranging we have

$$V_s = \frac{\frac{V_i}{LP_{atm}}\left(1+\frac{1}{2RT}Mv_{xm}^2\right)P_0 d}{ln\left[\left(1+\frac{1}{2RT}Mv_{xm}^2\right)P_0 d\right]-ln\left[LP_{atm}ln\left(\frac{1}{\gamma}+1\right)\right]-M_N} \qquad (19)$$

Eq. (19) also has the property that when $v_{xm} = 0$ Paschen's Law is returned. A graph of Eq. (19) with the parameters given in Table 2 is shown in Fig. 2.

TABLE 2: PARAMETERS FOR GRAPH IN FIG. 2

M = 0.029 kg/mol (air)	P_{atm} = 760 torr	d = 1.0 cm
T = 300 K	γ = 0.035 (Al)	V_i = 2.2 V (air)
v = 600 m/s	R = 8.314 J/K· mol	$L = 6.8 \times 10^{-6}$ cm

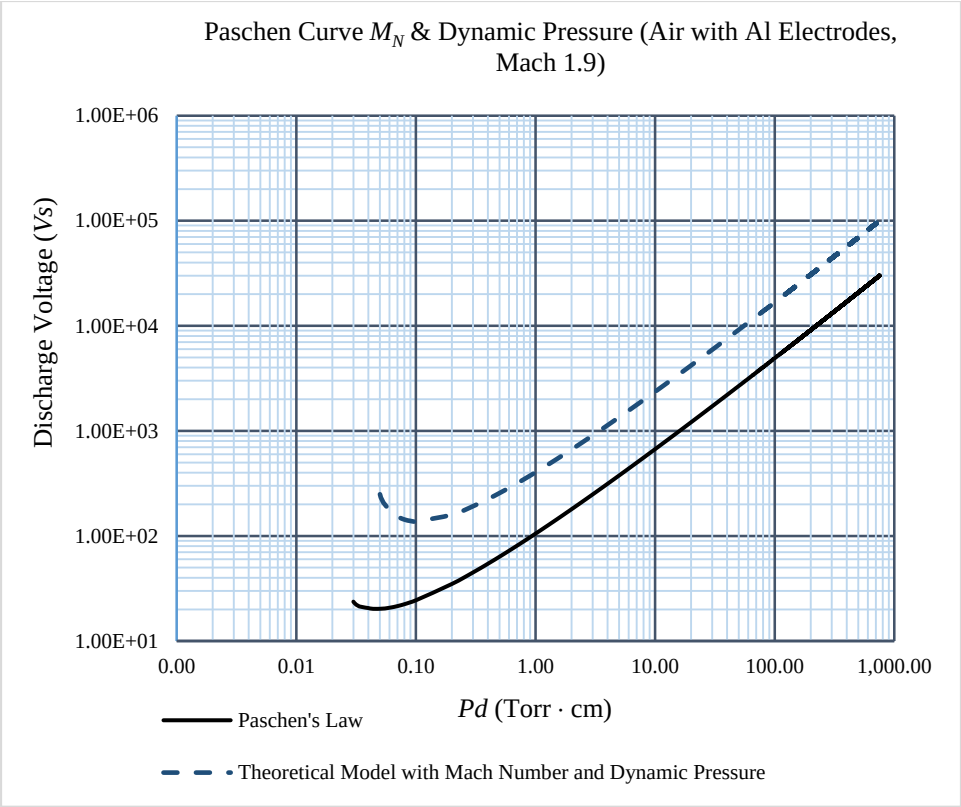

Fig. 2. Paschen's Law compared to the revised Mach number formulation with dynamic pressure terms.

This result looks promising since the separation of the curves is more pronounced at higher pressures. This will make the differentiation of the two curves from experimental data easier. Also of note is that the minimum sparking voltage is now a function of temperature as well as pressure, electrode separation, and mean gas velocity. For this study we assume that the ambient temperature is constant (~ 300 K).

$$V_s = f(P, d, T, v_{xm}) \tag{20}$$

D.An Apparent Effective Discharge Path

When air flows in a channel, a velocity profile is created [6]. This velocity profile is typically parabolic in shape with zero velocity at the channel walls and is maximum at the channel center. Velocity profile data from a Mach 1.5 wind tunnel experiment is graphed in Fig. 3 [7]. This velocity profile is linear across the center of the 4.4 cm wide channel because the length of the test section did not allow for the typical parabolic shape to develop [6].

A question arose as to how the velocity profile could relate to the minimum sparking voltage. A full scale print of this graph allowed measurement of the length along the velocity profile. This length was measured to be approximately 11.7 cm. Paschen's law, Eq.

(1) for an electrode gap of 4.4 cm, the theoretical model, Eq. (19) for a gap of 4.4 cm and Mach 1.5, and Paschen's law for a gap of 11.7 cm are graphed in Fig. 4.

The theoretical model curve at a gap of 4.4 cm and Mach 1.5 is a close match for Paschen's law curve for a gap of 11.7 cm at values of *Pd* above 1.0. It is not clear why this is so or why the curve deviates at values of *Pd* below 1.0. A hypothesis to explain this is that at higher values of *Pd* (higher pressures for fixed *d*) the motive behavior of gas molecules is mostly aerodynamic (molecules follow streamlines in the gas continuum) while at lower values of *Pd* (lower pressures for fixed *d*), the motive behavior of gas molecules is mostly ballistic (molecules follow kinematic paths) making aerodynamic continuum parameters less of an influence. For the higher values of *Pd* above 1.0 we hypothesize that the length along the velocity profile is an effective electrode separation, *d'*, caused by the flow of gas removing the electron – ion pairs between the electrodes. Analysis of other wind tunnel data with different channel widths and Mach numbers will be necessary to confirm this hypothesis.

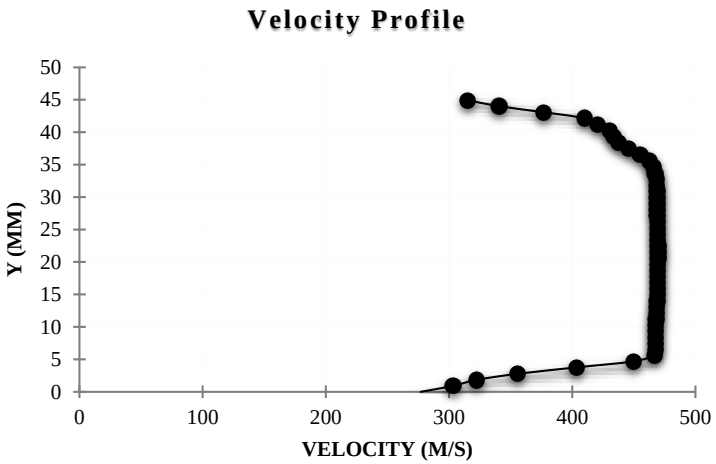

Fig. 3. Wind tunnel data with a channel width of 4.4 cm, a max velocity of Mach 1.5 and an air temperature of 300K.

To further evaluate this hypothesis, several Paschen curves were generated for electrode gap widths of 1.0 – 5.0 cm. These curves are shown in Fig. 5. It was noted that the sparking voltage, V_s, increased as expected but that the minimum sparking voltage was approximately the same for all the curves. This characteristic was similar to the two Paschen curves for d = 4.4 cm and d = 11.7 cm shown in Fig. 4. It was found that by removing the Mach number factor from the model equation, Eq. (19), the close correspondence between the model equation (with dynamic pressure terms only) and the Paschen curve for d = 11.7 cm was effected at all values of *Pd*. This is shown in Fig. 6. From inspection of Eq. (19) we hypothesize an expression for the effective electrode separation.

$$d' = \left(1 + \frac{1}{2}\frac{M}{RT} v_{xm}^2\right) d \qquad (21)$$

The result in Fig. 6 indicates that the dynamic pressure formulation of Paschen's law is

more accurate in evaluating the effect of gas velocity on the sparking voltage between two electrodes at all pressures.

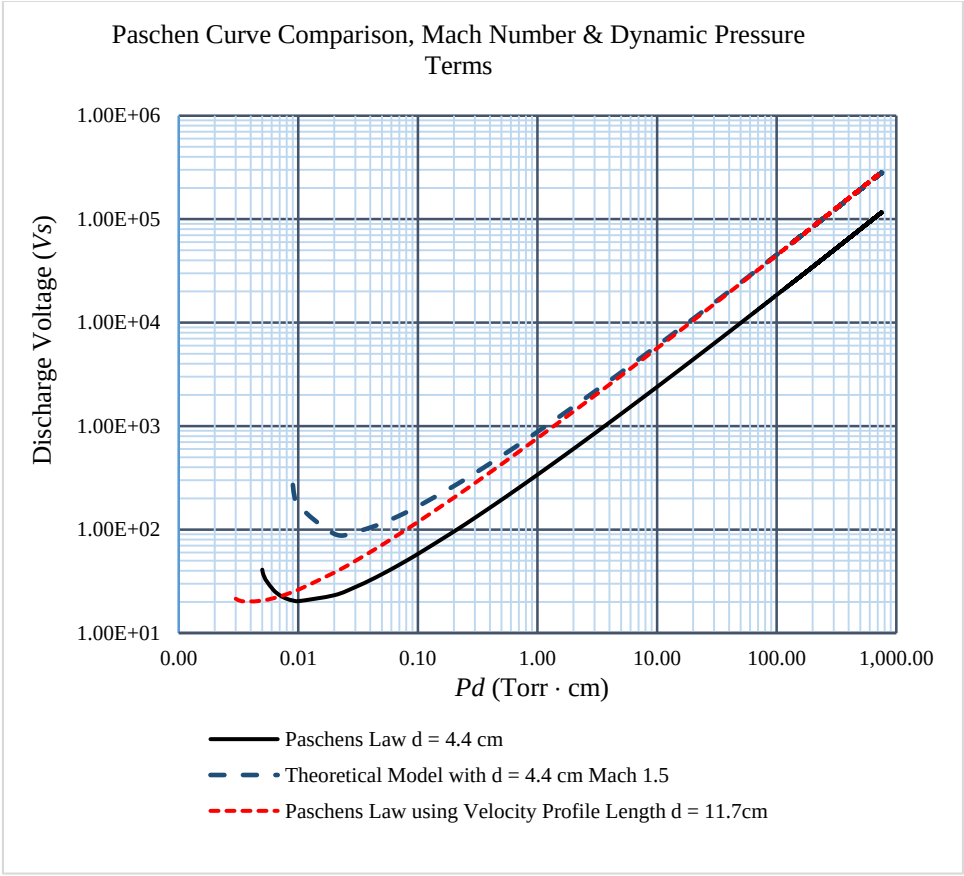

Fig. 4. Graph of Paschen's law for a 4.4 cm electrode separation, theoretical model for a gap of 4.4 cm and Mach 1.5, and Paschen's law for an electrode separation of 11.7 cm. The 11.7 cm is the length along the velocity profile in the wind tunnel test section. Air temperature is 300K.

III. Proposed Experiment

The Florida Center for Advanced Aero-Propulsion (FCAAP) of the University of Central Florida (UCF) is a co-investigating organization of this effort. This aerodynamic research center has a wind tunnel facility that will be modified for low Mach number discharge experiments to validate the theoretical model.

A. UCF CATER Wind Tunnel

The Center for Advanced Turbomachinery and Energy (CATER) supersonic wind tunnel, Figs. 7 and 8, at UCF, was manufactured by Aerolab Incorporated, of Laurel Maryland.

It is suitable for instruction, demonstration of basic principles of supersonic flow regime, flow visualization, and instrumentation research. It is fully representative of a "blowdown" wind tunnel facility.

Close to 18.9 cubic meters of air are available, at a nominal pressure of 300 psig (2,068 kPa). As a reference, typical mass flow rates when the tunnel is in operation are of the order of 2 kg/sec.

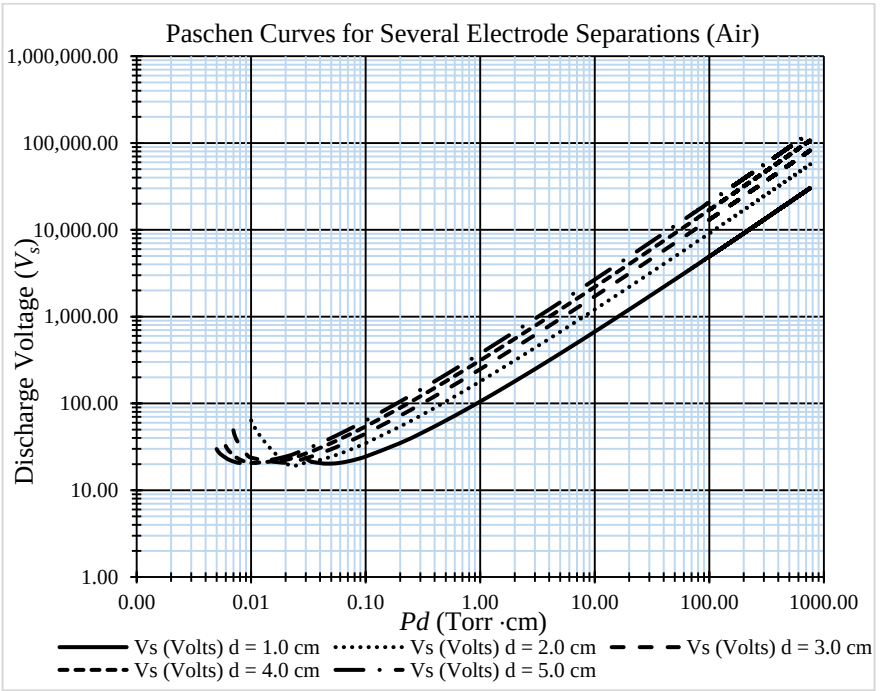

Fig. 5. Paschen curves for d = 1.0, 2.0, 3.0, 4.0, and 5.0 cm. Minimum sparking voltage is approximately the same for all curves.

The air flows into the tunnel "settling chamber" through a manual shut-off valve. The flow then enters the convergent part of a convergent-divergent nozzle, fabricated of steel sheet, which also functions as a shape change from a circular cross-section to rectangular. The latter part of the convergent section, the nozzle throat, and the divergent portion are formed using the wind tunnel test section sidewalls, with specially shaped upper and lower nozzle blocks.

The geometry of the nozzle, most importantly the throat-to-test section area ratio can be altered by a mechanical arm. The Mach number in the test section is dependent of the nozzle area ratio and can be varied from around 1.8 to around 2.8. A run will typically last around 1 minute for Mach 2 conditions in the test section. The test section, shown in Fig. 6, is nominally 10.16 cm in width by 10.16 cm in height in cross section. Its side walls are fabricated from glass which allows access for flow visualization. The electrodes will be supported by means of a rear strut (a "sting" support).

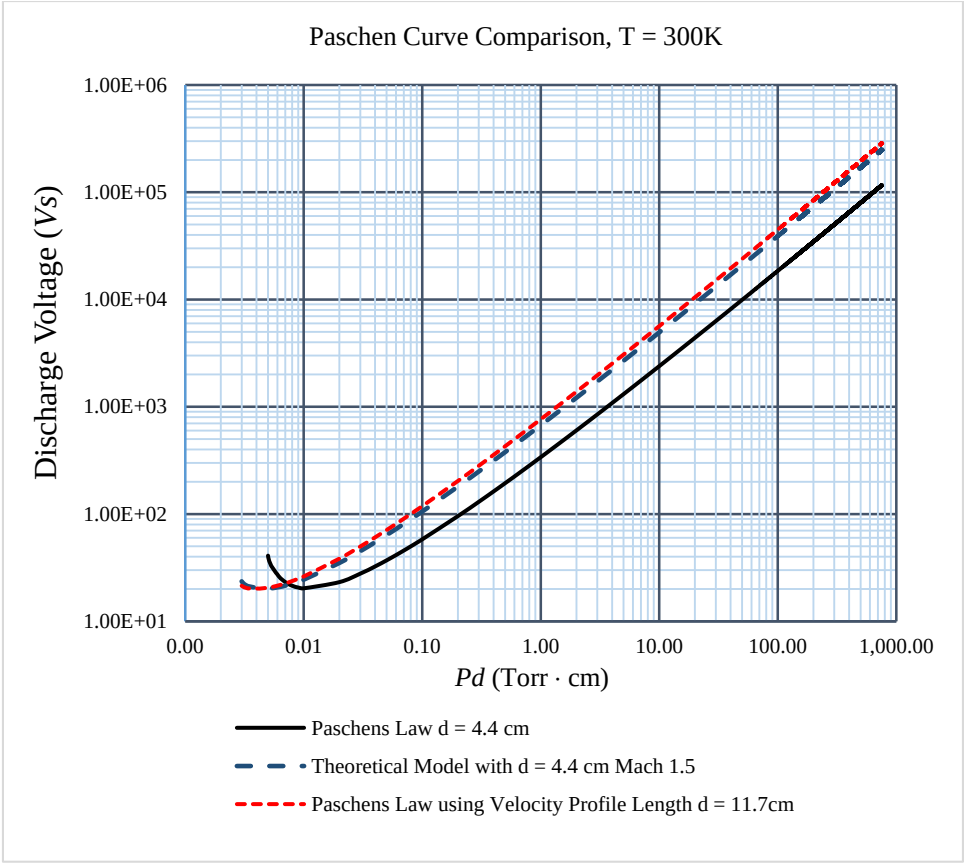

Fig. 6 Comparison of a Paschen curve (solid line) for d = 4.4 cm, the model equation with dynamic pressure terms only (large dashed line), and a Paschen curve using the approximate velocity profile length d = 11.7 cm (short dashed line) showing marked correspondence between the model equation and the Paschen curve calculated for the velocity profile length for all values of Pd. Air temperature is 300K.

Two methods are typically utilized in this facility for flow visualization. Both rely on refraction of light passing through regions of varying air density within the test section.

The Shadowgraph technique is the simplest and relies of direct projection of an initially parallel light beam onto a screen or camera lens. It can be shown that the intense variations are proportional to the second derivative of the flow density normal to the light beam. Variation in transmitted intensities are principally adjusted by the actual density gradient and the optical path lengths.

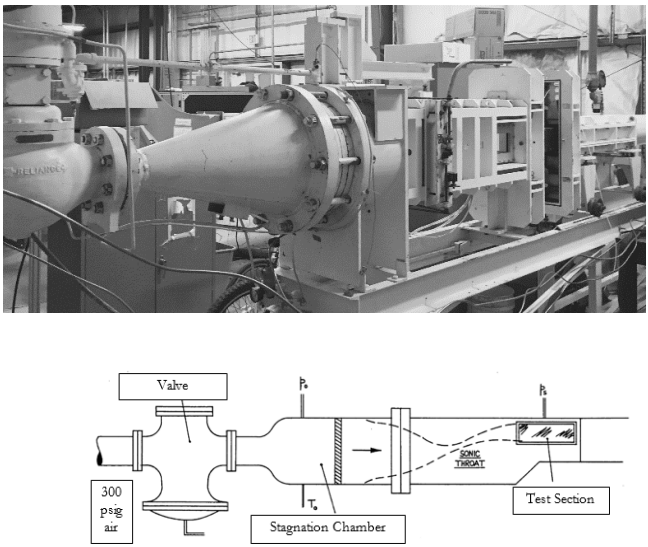

Fig. 7. The CATER supersonic wind tunnel at UCF.

Fig. 8. CATER wind tunnel test section.

The Schlieren technique involves focusing the light beam down to a small dot, partially intercepted by a "knife-edge". Small deflections of the light rays either closer to the knife-edge (more light blocked), or further away (less light blocked), will result in significant variations of the intensity of the transmitted light. Therefore this technique can be made extremely sensitive to density gradients.

Pressure is measured utilizing a pressure transducer. Usually, the reservoir pressure, stagnation chamber, and test section static pressures are measured in order to establish wind tunnel conditions. A single temperature measurement is made in the settling chamber utilizing a thermocouple.

B. Experiment Development to Date

The experiment will consist of two electrode plates placed 1.0 cm apart in the test section of the CATER wind tunnel. The test section, shown in Fig. 9, will be modified to mount

the electrodes and have other metal surfaces insulated to prevent discharge to those surfaces.

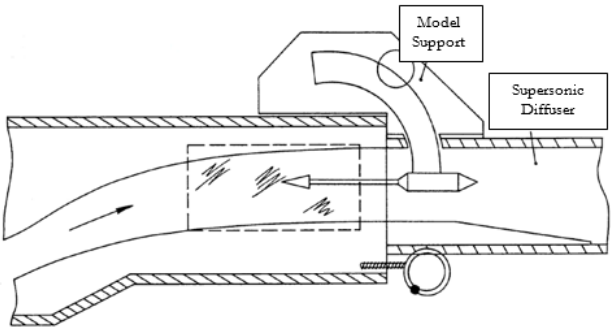

Fig. 9. Test section cross-sectional view

The electrode plates are being designed and fabricated by KSC. These plates will be made from T6061 aluminum plate stock with all edges rounded and surfaces polished to reduce any field concentration points. A notional design of an electrode plate is shown in Fig. 10. The dimensions of the 0.25 inch (0.635 cm) thick electrodes are 10 cm by 4.0 cm though these dimensions may change depending on test section requirements for mounting.

A Glassman 60 kV power supply will be used to energize one of the plates with the other grounded. Both voltage and current between the plates will be monitored. The UCF facility will also have flow visualization methods as described in Section III. A. Also, high speed video of the test section via the side windows will be performed to record discharges. A high-level schematic of this experiment is shown in Fig. 11.

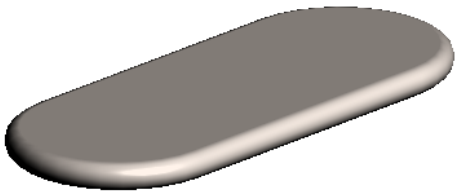

Fig. 10. Notional design of the electrode plates.

IV. Future Development Paths

There are several avenues for further theoretical development of the basic hypothesis that the discharge or sparking voltage calculated by Paschen's law is changed due to flow of the mediating gas between the electrodes.

One is to include a pressure dependence of the speed of sound. The speed of sound, is given by [8]

$$c = \sqrt{\gamma_a \frac{p}{\rho}} = \sqrt{\frac{\gamma_a RT}{M}} \tag{22}$$

Here γ_a is the ratio of specific heat at constant pressure, C_p, to the specific heat at constant volume, C_V, for air or $\gamma_a = C_p/C_v = 1.4$ and ρ is the gas density.

Another avenue for theoretical development is the fact that, for a velocity profile to exist, there must be a pressure gradient across the channel or dp/dy. In the wind tunnel experiment example above in Section II.D, the velocity profile was mostly linear except close to the channel walls, so dp/dy could be taken approximately as a constant. However, this is not usually the case if the channel is long enough to allow for a stable parabolic shaped velocity profile to develop.

Also we plan to further evaluate the effective discharge distance hypothesized in Section II.D. This hypothesis is based on a very limited data set so data from other wind tunnel experiments at different channel widths and gas velocities will need to be examined.

V. Conclusion

In this paper we have presented a re-derivation of Paschen's law that takes into account the flow of gas between the electrodes as a mitigating factor on the concentration of electron – ion pairs created by the potential. Aerodynamic properties such as the Mach number and dynamic pressure were used in this re-derivation and returned higher values of V_s, as would be expected if the concentration of electron – ion pairs were reduced by a rapid gas velocity.

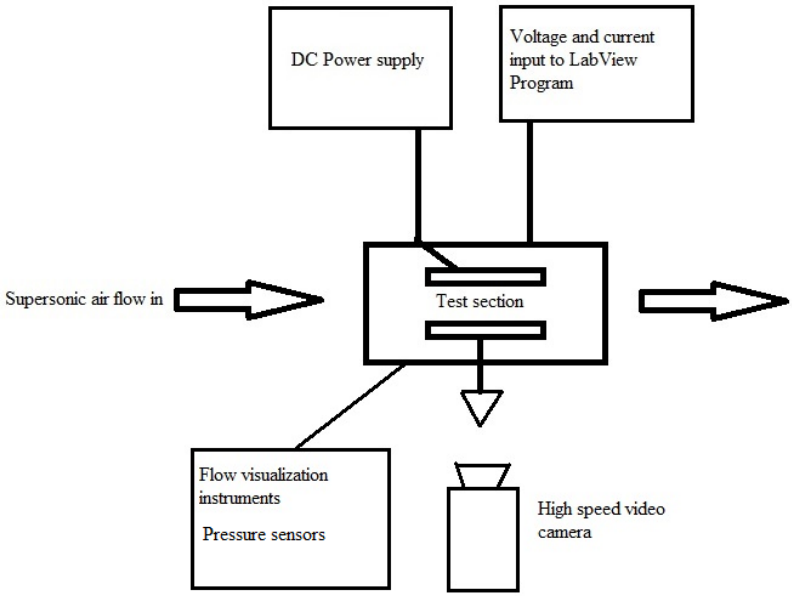

Fig. 11. A high level schematic of the CATER wind tunnel experiment to measure the electrical discharge characteristics of high speed flow past electrode plates.

Also, in a gas flow between the electrodes, an effective discharge distance was hypothesized to be the length of the resultant velocity profile at values of *Pd* above 1.0. With only dynamic pressure terms in the theoretical model, the resulting curve corresponds very well with the Paschen curve for a gap equal to the length of the velocity profile for all values of *Pd*. Further evaluation of this hypothesis is planned with larger wind tunnel data sets.

ACKNOWLEDGEMENTS

The authors would like to thank the NASA Science Innovation Fund (SIF) for their support of this work. Also special thanks to Mr. Michael Johansen and Mr. James Phillips for their reviews and helpful comments on this paper.

REFERENCES

[1] Friedrich Paschen "Ueber die zum Funkenübergang in Luft, Wasserstoff und Kohlensäure bei verschiedenen Drucken erforderliche Potentialdifferenz (On the potential difference required for spark initiation in air, hydrogen, and carbon dioxide at different pressures)". Annalen der Physik **273** (5): 69–75 (1889). *Bibcode:1889AnP...273...69P*. *doi:10.1002/andp.18892730505*.

[2] M. Hogue, C. Calle, ESPL Report, "Electrostatic Evaluation of the ARES I FTS Antenna Materials", ESPL-TR10-002, August 27, 2010. NASA, Kennedy Space Center.

[3] R. W. Fox, A. T. McDonald, *Introduction to Fluid Mechanics*, 2nd ed., John Wiley & Sons, 1978, p. 284.

[4] A. Von Hippel, *Molecular Science and Molecular Engineering*, (MIT Press, Wiley & Sons, 1959), pp 39-47.

[5] J. D. Cobine, *Gaseous Conductors: Theory and Engineering Applications*, Dover, 1993, p. 159, Table 7.3.

[6] http://www.uio.no/studier/emner/matnat/math/MEK4450/h11/undervisningsmateriale/modul-5/Pipeflow_intro.pdf

[7] Velocity profile data provided by Dr. K. Ahmed/UCF, 2-17-2016.

[8] R. W. Fox, A. T. McDonald, *Introduction to Fluid Mechanics*, 2nd ed., John Wiley & Sons, 1978, p. 496.